Presented at the 22nd European Photovoltaic Solar Energy Conference and Exhibition, 3 - 7 September 2007, Milan, Italy.

EFFICIENT UPCONVERSION SYSTEMS FOR SILICON SOLAR CELLS

P. Löper[1], J. C. Goldschmidt[1], M. Peters[1], D. Biner[2], K. Krämer[2], O. Schultz[1], S. W. Glunz[1], J. Luther[1]
[1] Fraunhofer Institute for Solar Energy Systems, Heidenhofstr. 2, 79110 Freiburg, Germany
[2] University of Berne, Freiestrasse 3, 3012 Bern, Switzerland
Phone: +49 (0) 761 4588 5263, Fax: + 49 (0) 4588 9250, Email: philipp.loeper@ise.fraunhofer.de

ABSTRACT: Frequency upconversion of sub-bandgap photons is one approach to push the efficiency limit of solar cells with one bandgap. A highly efficient upconversion system is Erbium doped $NaYF_4$. In this paper we present photoluminescence studies on $NaYF_4$ with 10%, 20% and 30% Erbium doping. We show experimental results of an upconversion system consisting of an upconverting powder on a bifacial silicon solar cell. The system has a quantum efficiency of $2.5 \cdot 10^{-3}$% at 1520nm wavelength. We model the efficiency enhancement of an upconversion system by spectral concentration with fluorescent dyes. To enhance the upconversion efficiency, fluorescent dyes can be used for spectral concentration. Our theoretical calculation show that an eightfold increase in upconversion efficiency is within reach.
Keywords: Upconversion, Downshifting, Rare Earth, Photoluminescence, Spectroscopy

1 MOTIVATION

Silicon solar cells lose at least 20% of the incident radiation power because photons with energy below the bandgap are transmitted. Frequency upconversion of sub-bandgap light is an approach to overcome this principal problem. The theoretical efficiency limit is pushed from close to 30% [1] to 40.2% [2] for a silicon solar cell with an upconverter illuminated by non-concentrated light. Figure 1 shows a possible design of an upconversion system. Similar upconversion systems have been realized by Shalav [3] and Strümpel [4].

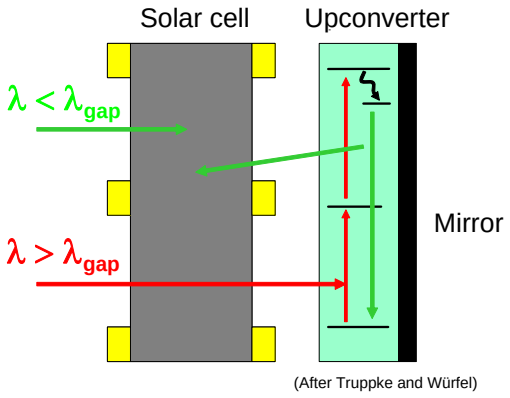

Figure 1: Bifacial solar cell with an upconverter on its rear side. Sub-bandgap photons are transmitted through the solar cell but absorbed in the upconverter which is excited successively. By recombination to the ground state, the upconverter emits a photon which can be absorbed by the solar cell.

2 LUMINESCENCE CHARACTERISTICS

2.1 Comparison of Absorption and Photoluminescence

Very suitable as an upconverter are Rare Earth based materials like $NaYF_4$ [5], which was used in our experiments. Rare earths, especially trivalent Erbium, exhibit 4*f*-levels which are very conveniently spaced for upconversion for solar cells.

One advantage of $NaYF_4$ is its very low maximum phonon energy. Excited states may decay nonradiatively by multiple emission of phonons to the next lower lying state. The maximum phonon energy thus determines the nonradiative decay of an excited state.

Figure 2 shows the absorption and photoluminescence (PL) of $NaYF_4$: 20% Er^{3+} in a binding agent. $NaYF_4$ cannot be synthesized as a bulk but only as a microcrystalline powder. Therefore, a binding agent is needed to apply the powder on a solar cell. The spectral features of the absorption spectrum for wavelengths λ >500nm which are not due to the binding agent coincide with the PL emissions. Compared to the absorption peaks, the PL emissions are slighty shifted to longer wavelengths due to the stokes shift. The highest PL emission, excited via at least three absorptions, is at 545nm and can be seen in the spectrum. PL emissions with wavelengths λ <500nm are not visible in the spectrum. They are very weak as they involve four upconversion steps. The broad absorption of $NaYF_4$: Er^{3+} at 1520nm can be used to upconvert sub-bandgap photons. The luminescence at 980nm is adequate to illuminate a silicon solar cell because the latter exhibits high quantum efficiencies in this region. The PL emissions can be assigned to the energy levels of trivalent Erbium. The energy levels of Er^{3+} are shown schematically in Figure 3 together with their radiative decays to the ground state and the most probable

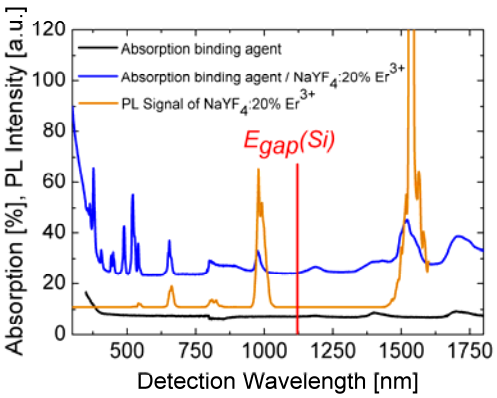

Figure 2: Absorption and Photoluminescence of $NaYF_4$: 20% Er^{3+}. The PL spectrum was recorded at an excitation wavelength of 1523nm. The PL emission at 980nm lies above the bandgap of silicon.

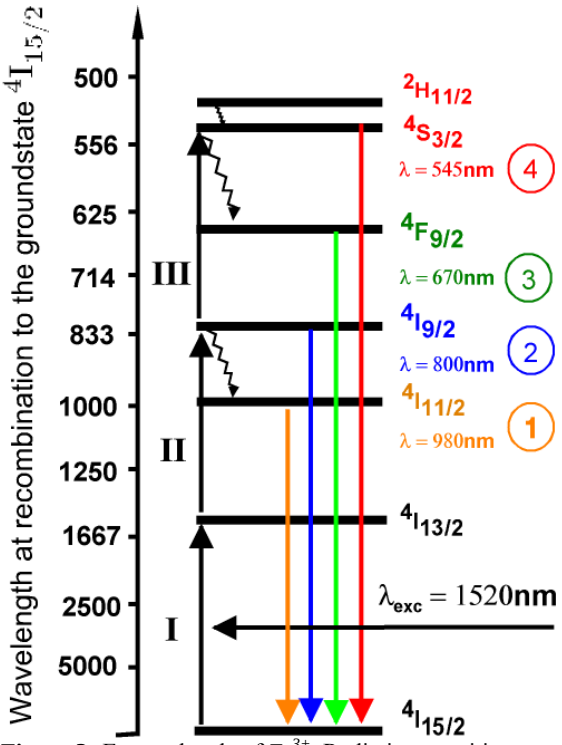

Figure 3: Energy levels of Er^{3+}. Radiative transitions are indicated by solid arrows, non-radiative transitions by wavy arrows.

non-radiative decays. If pumped at 1520nm, Er^{3+} is successively excited to the $^4I_{9/2}$ state via the transitions $^4I_{15/2} \rightarrow {}^4I_{13/2} \rightarrow {}^4I_{9/2}$, represented in figure 3 by black solid arrows. This may be followed by further upconversion to the $^4S_{3/2}$ or $^4H_{11/2}$ states,
decay to the ground state or decay to the next lower lying state $^4I_{11/2}$. The radiative transitions to the groundstate $^4I_{9/2} \rightarrow {}^4I_{15/2}$ and $^4I_{11/2} \rightarrow {}^4I_{15/2}$ are best suited to illuminate a silicon solar cell because the latter shows high quantum efficiencies at 800nm and 980nm. Further upconversion to higher levels would involve another photon but would not lead to an increased solar cell response and is therefore not desired.

2.2 Upconversion Mechanisms

The main upconversion mechanisms via metastable states are "Excited State Absorption" (ESA) and "Energy Transfer Upconversion" (ETU) [6].

An ESA process is the transition of one atom from an excited state to a higher excited state by absorption of a photon.

ETU involves two atoms in an excited state. One atom transfers its energy to the other and relaxes, while the latter is further excited.

In case of equally spaced energy levels, the population N_k of a level k, excited by k upconversion steps, is for

ESA: $N_k \propto N_{k-1} \cdot I_{exc}$

ETU: $N_k \propto N_{k-1} \cdot N_1$

I_{exc} denotes the excitation intensity at the absorption wavelength. Without loss of generality, in this example for ETU the transition from the *first* excited to the ground state couples resonantly with the transition from the (*k-1*)th to the *k*th state. In general, *any two* transitions with an appropriate spectral overlap can couple.
The populations N_{k-1} and N_1 depend linearly on the excitation intensity I_{exc}. Iteration leads to [7]:

$$N_k \propto I_{exc}^k$$

If other processes than radiative recombination to the ground state from level k are neglected, the exponent k reflects the order of the process, i.e. the number of photons involved. For example, the upconversion photoluminescence (PL) intensity $I_{PL,800nm}$ at 800nm would depend quadratically on the excitation intensity

$$I_{PL,800\,nm} \propto N(^4I_{13/2}) \cdot I_{exc} \propto I_{exc}^2$$

With non-radiative relaxation, upconversion to higher levels, radiative relaxation to others than the ground state, excitation migration or cross relaxation, an excited atom is less likely to relax radiatively to the groundstate. Consequently, the PL exhibits a lower exponent of power dependence.
Excitation migration and cross relaxation are the inverse process to ETU. One atom relaxes and transfers its excitation to a neighboring one. Excitation migration refers to an event where the excitation only migrates, but the densities of the excited states remain constant. Cross relaxation means a decrease in the density of a higher excited states, populating a lower (e.g. first) excited state. In both processes, the coupling between two atoms can be either radiatively, obeying a $1/d^2$ [6] law, or non-radiatively via dipole-dipole interaction and thus decreasing like $1/d^6$ with interatomar distance d. Therefore, ETU and cross relaxation strongly depend on the dopand concentration.

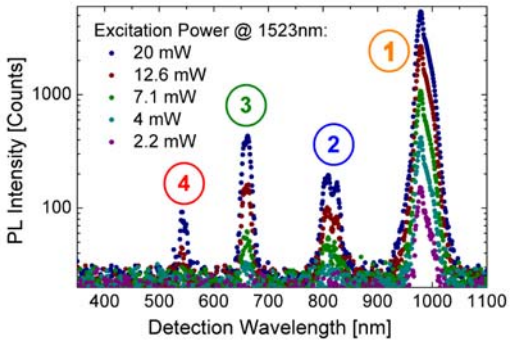

Figure 4: PL spectrum of $NaYF_4$: 20% Er^{3+} excited at λ=1523nm. The laser power was varied from 0.71mW to 19.95mW. The excited volume was constant. The transitions are labelled according to figure 3.

PL spectra were recorded at various excitation intensities in order to investigate the underlying upconversion dynamics and the optimum dopand concentration. Figure 4 shows upconversion PL spectra from $NaYF_4$: 20%Er^{3+}, recorded at different incident intensities. The laser power was varied from 0.71mW to 19.95mW at constant focus size. Figure 5 shows the integrated intensity of each luminescence peak as a function of excitation power.
For several regimes the exponents were determined by fitting a function $I_{PL}=const\cdot(P_{exc}-P_0)^m + I_{PL,0}$ to the data. I_{PL} denotes the PL intensity and P_{exc} the excitation power. The ordinate P_0 accounts for the onset of a certain power dependence regime and $I_{PL,0}$ for an offset. All Peak were fitted from P_{exc}=2.51mW to 10.0mW and from

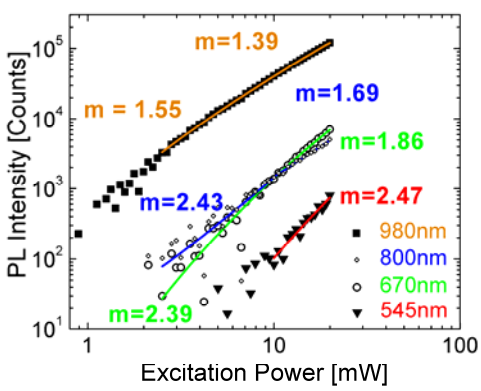

Figure 5: Power dependence of the upconversion emissions of $NaYF_4$: Er^{3+}20%, measured at λ_{exc}=1523nm. The colours are chosen according to figure 3.

P_{exc}=10.0mW to 19.95mW. Figure 5 shows the results in double logarithmic representation. The exponent m represents the slope of the fit curves in the double logarithmic plot.

In the low power regime the 980nm ($^4I_{11/2}$), 800nm ($^4I_{9/2}$) and 670nm ($^4F_{9/2}$) emissions show exponents m=1.55, 2.43 and 2.39, respectively.
This indicates a two-step process of the 980nm luminescence and a three-step process of both the 800nm and 670nm emission. The 800nm luminescence is emitted from the state $^4I_{9/2}$ which is populated via two upconversion steps. The exponent m > 2 indicates that this level is considerably fed by decay of the $^4F_{9/2}$ state. The $^4F_{9/2}$ state in turn is fed by the decay of $^4S_{3/2}$ and thus a third-step process, in accordance with its exponent of 2.39.

In the high power regime, the 980nm ($^4I_{11/2}$), 800nm ($^4I_{9/2}$), 670nm ($^4F_{9/2}$) and 545nm ($^4S_{3/2}$) emissions show the exponents m=1.39, 1.69, 1.86 and 2.47, respectively. This indicates a two-step process for the 980nm and 800nm emissions. With higher excited state densities, cross relaxations become more competitive with upconversion steps. Hence, the exponents of the 800nm *and* 670nm emissions are lower, compared to the low power regime. The higher exponent of the 800nm luminescence compared to the one of the 980nm emission again indicates a decay route $^4F_{9/2} \rightarrow {}^4I_{9/2}$.

The 545nm emission shows an exponent m=2.47 in the high power regime, which is in accordance with a three step process. At low powers the 545nm peak was too noisy to be evaluated. Shalav measured m=1.50, 1.55, 1.87 and 3.0 as exponents for the 980nm, 800nm, 670nm and 545nm emission in the high power regime. But as the illuminated volume in the two experiments is unknown, no exact comparison can be made.

2.3. Influence of doping concentration

To determine the optimum dopant concentration in the host crystal $NaYF_4$, the luminescence intensities of $NaYF_4$ with 10%, 20%, 30% Er^{3+} doping were recorded and the integrated luminescence of every peak calculated. Figure 6 shows the results normalized to the brightest sample. The 20% doped sample clearly yields the most efficient upconversion. The 30% doped sample

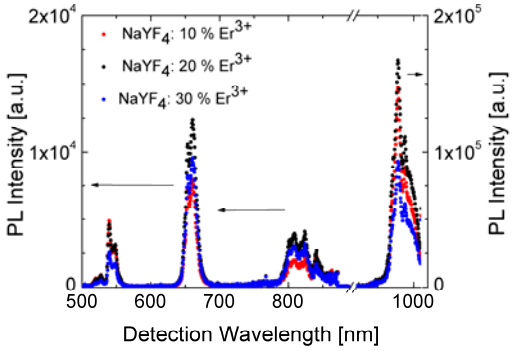

Figure 6: Spectra of $NaYF_4$ based upconverters, doped with 10%, 20% and 30% of Erbium^{3+}. The Peak at 980nm belongs to a different scale.

shows much lower emission at 545nm compared to the 10% and 20% samples. As explained in section 2.2, at higher doping the coupling with neighbour dopants increases, leading to more cross relaxation and excitation migration. The decrease in 545nm luminescence can be explained with two cross relaxation decay routes of the 545nm emitting $^4S_{3/2}$ state (see figure 3): $^4S_{3/2} + {}^4I_{X/2} \rightarrow {}^4I_{9/2} + {}^4I_{Y/2}$, where $X=15$ or $X=13$ and $Y=13$ or $Y=9$, respectively. Consequently, the 800nm and 1520nm emitting energy levels are populated at the expense of 545nm emission. The stronger emission at 800nm of the 30% sample can also be seen in figure 7.

At 980nm and 545nm, the 10% doped sample emits almost as strong as the 20% doped sample. To maximize the 800nm and 980nm emissions at the cost of the other emissions, more samples with different doping concentrations still have to be investigated.

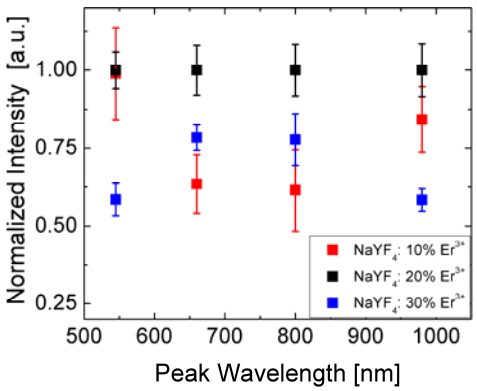

Figure 7: Comparison of *$NaYF_4$* based upconverters, doped with 10%, 20% and 30% of Er^{3+}. For every sample, the detected luminescence intensity is integrated over every peak and normalised to the brightest sample.

3 UPCONVERSION SOLAR CELL SYSTEM

The upconversion luminescence of trivalent Erbium can be used to illuminate a solar cell. A system consisting of a bifacial silicon solar cell and an upconverter was constructed as illustrated in Figure 1. The bifacial cell had an interdigitating pn-structure with both grids on one side. The upconverter was applied to the grid-free surface

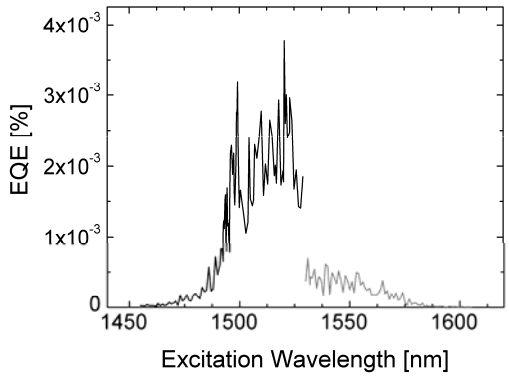

Figure 8: Spectral response of a bifacial silicon solar cell with $NaYF_4$: 20% Er^{3+} as an upconverter, excited by a collimated laser beam with 15mW optical power. From 1530nm to 1605nm the measurement has to be repeated.

and the cell contacted from the other side, as depicted in figure 9. Acrylic paint was used as a binding agent for the microcrystalline $NaYF_4$: 20% Er^{3+}. The cell was illuminated from the grid covered side and a diffuse mirror was attached to the rear (unilluminated) side of the system behind the upconverter. The spectral response was measured using a tunable Santec ECL-210 laser at about 10mW optical power. The light was collimated and chopped at 5Hz and a lock-in amplifier used to measure the short circuit current of the solar cell. No white bias light was used. Figure 8 shows the quantum efficiency, calculated as the ratio of the short circuit currents of the upconversion system and a GaSb reference cell. The maximum quantum efficiency is $2.5 \cdot 10^{-3}$ % between 1500nm and 1530nm.

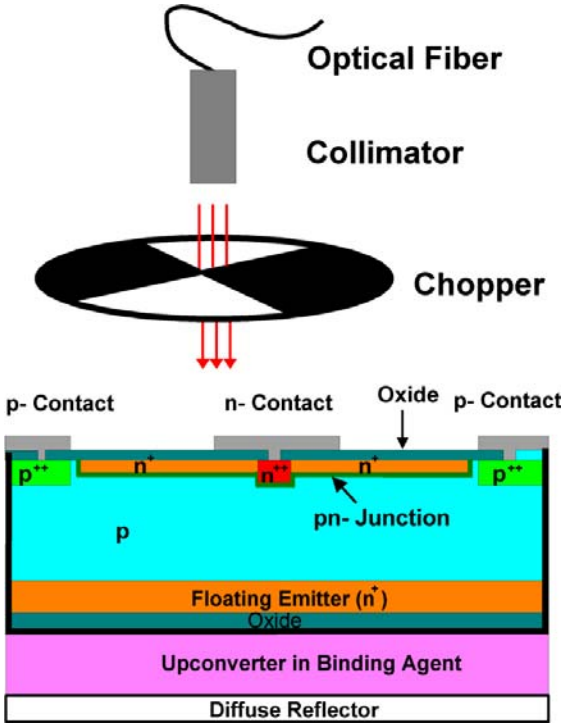

Figure 9: Experimental setup for the spectral response measurement. The upconverter is optically coupled to the solar cell but electrically isolated.

Shalav reported 3.4 % quantum efficiency [8] for laser illumination at 1523nm and 6mW.

The discontinuity in the measured spectral response is due to problems with the detection electronics. From 1530nm to 1605nm wavelength, the measurement has to be repeated. For excitation wavelengths $1445nm<\lambda_{exc}<1530nm$, the qualitative form of the spectral response is confirmed by photoluminescence excitation spectra of the same upconverter. Figure 10 shows the integrated peak intensities of the four emissions at 980nm, 800nm, 670nm and 545nm at excitation wavelengths from 1445nm to 1530nm. Maxima can be distinguished at 1497nm, 1510nm and 1520nm. The luminescence excitation spectrum matches the spectral response of the solar cell.

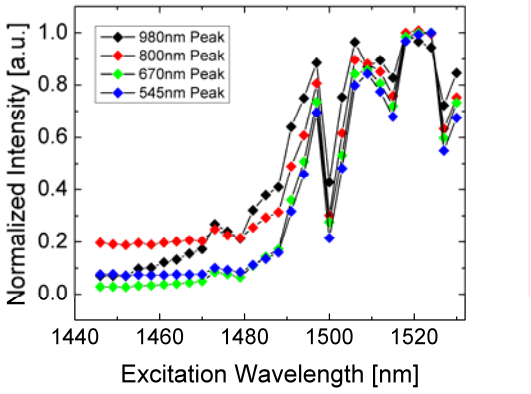

Figure 10: Excitation Spectrum of $NaYF_4$: 20% Er^{3+}. For every peak, the PL signal is integrated and normalized to its maximum for better comparison.

4 ENHANCING SYSTEM EFFICIENCY

The major problem of rare earth based upconverters like Erbium doped $NaYF_4$ is the small absorption range of the rare earth dopand. To overcome this limitation, Strümpel [4] suggested the combination of an upconverter with a fluorescent material. The fluorescent material should absorb all photons with wavelengths between the

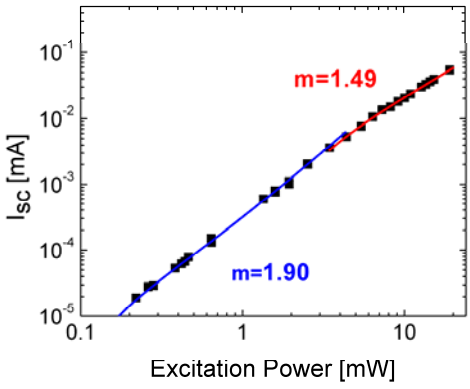

Figure 11: Power dependence of the short circuit current I_{sc} of the upconversion system consisting of a bifacial silicon solar cell and a $NaYF_4$: 20% Er^{3+} based upconverter. The exciation wavelength was 1520.5nm.

bandgap of the solar cell and the absorption of the upconverter and emit in the narrow absorption range of the upconverting material. Because the solar photon density over a broad spectral range is funnelled to a smaller range, we call this process spectral concentration. This approach increases the upconversion efficiency significantly by two mechanisms: Firstly, more light is absorbed that is potentially upconvertible. Secondly, the photon density in the absorption range of the upconverter is increased.

Figure 11 shows the solar cell response on excitation power of the upconversion system described above. The function $J_{sc}=const\cdot (P_{exc}-P_0)^m+J_{sc,0}$ was fitted to the data for low ($0.21\text{mW}\le P_{exc}\le 3.46\text{mW}$) and high ($4.38\text{mW}\le P_{exc}\le 19.07\text{mW}$) excitation powers. J_{sc} denotes the solar cell short circuit current and P_{exc} the excitation power. The ordinate P_0 accounts for the onset of a certain power dependence regime and $J_{sc,0}$ for an offset. As the solar cell detects all upconversion luminescence, its response represents a weighted averaged of all upconversion luminescence peaks. For low powers the solar cell short circuit current J_{sc} depends almost quadratically (m=1.9) on excitation power. For higher excitation powers an exponent m=1.49 was determined which is due to saturation effects. Shalav [3] reported slightly higher values of m=1.57 for low and m=2.0 for high powers. In case of solar illumination, the low power approximation is valid and therefore a quadratic power dependence can be assumed.

A quadractic dependence of J_{sc} leads to a linear dependence of the external quantum efficiency on incident power: $EQE_{UC} \sim J_{sc}/P_{exc}=P^2_{exc}/P_{exc}=P_{exc}$

We define the upconversion efficiency η_{UC} of an upconverter system as the fraction of upconverted photons ϕ_{UC} emitted above the bandgap and the number of photons ϕ incident on the upconverting system with energies below the bandgap.

$$\eta_{UC} := \frac{\int_0^{\lambda_{gap}} \phi_{UC}(\lambda)d\lambda}{\int_{\lambda_{gap}}^{\infty} \phi(\lambda)d\lambda} = \frac{\int_{\lambda_{gap}}^{\infty} EQE_{UC}(\lambda)\cdot\phi(\lambda)d\lambda}{\int_{\lambda_{gap}}^{\infty} \phi(\lambda)d\lambda}$$

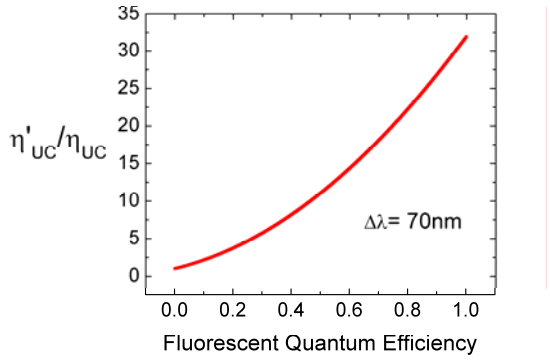

Figure 12: Ratio of the upconversion efficiency of a combined system, η'_{UC}, to the upconversion efficiency of a single upconverter, η_{UC}. A quantum efficiency of the fluorescent material QE_F = 50% was assumed. $\Delta\lambda$=70nm is the width of the upconverters aborption range, which is supposed to match the emission range of the fluorescent material.

This definition has the advantages that it depicts the information relevant for the application of solar cell efficiency enhancement.

To compare the effect of spectral concentration on the upconversion efficiency we calculate the relation of the latter of an upconverter combined with a fluorescent material as described above, η'_{UC}, to the upconversion efficiency of an upconverter alone, η_{UC}. For simplicity, EQE_{UC} is assumed to explicitly depend only on photon density, but not on wavelength. Important is the assumption, that any electron in the first excited state ($^4I_{13/2}$ for Er^{3+}) can be excited to the next higher state by any photon emitted by the fluorescent material. The total quantum efficiency for the photons absorbed by the fluorescent material is the product of the EQE_{UC} of the upconverter in its absorption range $\lambda_{min}\le\lambda\le\lambda_{max}$ and the quantum efficiency QE_F of the fluorescent material (which is assumed to be constant for simplicity).

The efficiency η'_{UC} of the system with spectral concentration is

$$\eta'_{UC} = (\phi_{Integral})^{-1}\, EQE(\phi)\left(\int_{\lambda_{gap}}^{\lambda_{min}} QE_F\ \phi(\lambda)d\lambda + \int_{\lambda_{min}}^{\lambda_{max}} \phi(\lambda)\,d\lambda\right)$$

$$= (\phi_{Integral})^{-1}\, k\left(\int_{\lambda_{gap}}^{\lambda_{min}} QE_F\phi(\lambda)d\lambda + \int_{\lambda_{min}}^{\lambda_{max}} \phi(\lambda)d\lambda\right)^2$$

$$\phi_{Integral} = \int_{\lambda_{gap}}^{\infty} \phi(\lambda)d\lambda$$

The efficiency enhancement due to spectral concentration relative to a single upconverter is

$$\frac{\eta'_{UC}}{\eta_{UC}} = \frac{\left(\int_{\lambda_{gap}}^{\lambda_{min}} QE_F\ \phi_{Sun}(\lambda)d\lambda + \int_{\lambda_{min}}^{\lambda_{max}} \phi_{Sun}(\lambda)\,d\lambda\right)^2}{\left(\int_{\lambda_{min}}^{\lambda_{max}} \phi_{Sun}(\lambda)\,d\lambda\right)^2}$$

Figure 12 shows the increase in upconversion efficiency due to the fluorescent material and spectral concentration dependent on the quantum efficiency QE_F when the system is illuminated with the AM1.5G spectrum. Even with low quantum efficiencies of the fluorescent material a strong enhancement in upconversion efficiency is reachable. The calculation was done for a 70nm broad absorption range of 1480nm-1550nm, according to the Er^{3+} absorption range. Commercial nanocrystals have a fluorescent quantum efficiency of about 50%, but an emission range broader than the Erbium absorption. By matching the emission of a fluorescent material to the Erbium absorption, an eightfold increase in upconversion efficiency is within reach.

5 SUMMARY

We presented photoluminescence studies on $NaYF_4$ based upconverters and upconversion solar cell systems. The upconversion mechanisms were studied and found to comply with theorectical expectations. Doping concentrations of 10%, 20% and 30% were compared with respect to their applicability to solar cells. An Erbium content of 20% yielded the best results but has yet to be optimized. The material $NaYF_4$: 20% Er^{3+} shows promising characteristics to extend the spectral response of a silicon solar cell down to 1530nm. A

silicon solar cell with a $NaYF_4$: 20% Er^{3+} upconverter exhibited a quantum efficiency of $2.5 \cdot 10^{-3}$% for wavelengths between 1500nm and 1530nm. To increase the upconversion efficiency, we modelled spectral concentration by the combination of a fluorescent dye with an upconverter. According to our model, an eightfold increase in upconversion efficiency seems to be within reach.

6 ACKNOWLEDGMENTS

The authors thank Elisabeth Schaeffer, Michael Rauer, Anna Walter and Katarzyna Bialecka and for their support and fruitful discussions.

The presented work is partly financed by the German Research Foundation within the Nanosolar project and by the German Federal Ministry of Education and Research within the Nanovolt project. J. C. Goldschmidt gratefully acknowledges the scholarship support from the Deutsche Bundesstiftung Umwelt, and the ideational support from the Heinrich-Böll Stiftung and the German National Academic Foundation.

[1] W. Shockley and H.J. Queisser, Journal of Applied Physics 32 (1961) 510.
[2] T. Trupke, A. Shalav, B.S. Richards, P. Würfel and M.A. Green, Solar Energy Materials & Solar Cells 90 (2006) 3327.
[3] A. Shalav, B.S. Richards, T. Trupke, K.W. Krämer and H.U. Güdel, Applied Physics Letters 86 (2005) 13505.
[4] C. Strümpel, M. McCann, G. Beaucarneb, V. Arkhipov, A. Slaoui, V. Svrcek, C. del Canizo and I. Tobias, Solar Energy Materials & Solar Cells 91 (2007) 238.
[5] K.W. Krämer, D. Biner, G. Frei, H.U. Güdel, M.P. Hehlen and S.R. Lüthi, Chemical Materials 16 (2004) 1244.
[6] F. Auzel, Chemical Review 104 (2004) 139.
[7] M. Pollnau, D.R. Gamelin, S.R. Lüthi, H.U. Güdel and M.P. Hehlen, Physical Review B (Condensed Matter) 61 (2000) 3337.
[8] A. Shalav, B.S. Richards, K. Krämer and G. H., Proceedings of the 31st IEEE Photovoltaic Specialists Conference, Florida, USA (2005) 114.